Hindawi
Journal of Sensors
Volume 2022, Article ID 3866692, 9 pages
https://doi.org/10.1155/2022/3866692

Research Article

Influence of Dielectric Loss on RF Performance of Microstrip Multi-Resonant Circuits

Huating Tu,[1] **Hong Hong**,[2] **Yaya Zhang**,[3] **Liang Zhou**,[1] **and Xiaoou Li**[1]

[1]*College of Medical Instruments, Shanghai University of Medicine & Health Sciences, Shanghai 201318, China*
[2]*School of Materials Science and Engineering, Shanghai Institute of Technology, Shanghai 201418, China*
[3]*Shanghai Collaborative Innovation Center for High Performance Fiber Composites, Donghua University, Shanghai 201620, China*

Correspondence should be addressed to Xiaoou Li; lixo@sumhs.edu.cn

Received 29 March 2022; Revised 30 May 2022; Accepted 30 June 2022; Published 22 July 2022

Academic Editor: Wen-Ming Chen

Nowadays, fabric-based antennas, resonators, and sensors are attracting significant attention due to their excellent comfortability and flexibility compared with the rigid commercial printed circuit boards (PCBs). Both the dielectric constant (ε_r) and dielectric loss tangent (tan δ) of substrate materials have a great influence on their frequency response characteristics. However, the effect of dielectric loss is usually ignored, since traditional radio frequency (RF) devices are fabricated on commercial PCBs with much lower tan δ. As the differences of dielectric loss vary widely with different fabric materials, it is of great significance to explore the influence of dielectric loss on the frequency response characteristics. Therefore, this paper systematically studied the influence of substrate properties on RF performance of microstrip multiresonator. Firstly, the models of microstrip multiresonators with different ε_r and tan δ were created by HFSS simulation. By parametrically sweeping, it showed that the tan δ was the key factor for the notch depth. And the larger the tan δ, the bigger the electromagnetic loss of the material, resulting in a smaller notch depth of the resonator. Then, three representative materials with different orders of magnitude of tan δ (AD-450: 0.002, FR-4: 0.015, and denim fabric: 0.114) were chosen to verify the simulation. The results showed that the common fabric-based resonator has poor RF characteristics for their big dielectric loss compared with those of commercial PCBs. This study is of great significance for designing wearable electronic devices with flexible substrate materials with large dielectric loss.

1. Introduction

Nowadays, increasingly flexible materials such as fabrics [1, 2], papers [3, 4], and plastic films [5] are replacing traditional PCBs, to be used in wearable antennas, resonators, sensors, and so on. As one of the typical circuits within the above applications, the RF performances of U-shaped multiresonator were widely discussed. Generally speaking, the dielectric constant and loss tangent are vital factors to be considered when designing the multiresonator, which will affect the resonant frequency and notch depth significantly.

However, the influence of dielectric loss was usually ignored as the dielectric constant and thickness of substrates can change the resonant frequency, bandwidth, and gain to a large extent [6, 7]. Yves-Thierry et al. [8] pointed out that thin substrates of high dielectric constant lead to poor radiation and narrow bandwidth. On the other hand, since traditional RF devices are fabricated on commercial PCBs with much lower tan δ, the effect of dielectric loss was usually ignored. As shown in Table 1, the tan δ of most PCBs are lower than 0.002 in chipless applications [9–12]. However, it is an order of magnitude higher (>0.01) for flexible materials such as papers, plastics, or common fabrics. Therefore, studying the effect of dielectric loss on the RF performance is necessary because classical PCB-based circuits may not be suitable for most flexible materials such as fabrics. In addition, Islam and Karmakar [13] obtained the relationship between the attenuation and tan δ at 2.45 GHz by simulation (Figure 1). The results showed that the attenuation decreased sharply at first and then slowly with the increase of tan δ. However, the dielectric loss was discussed from a simulation perspective, and it lacks theoretical and experimental basis. In summary,

Table 1: Parameters of PCBs used in chipless tags. The tan δ of most commercial PCBs are lower than 0.002, while it is much higher for flexible materials such as papers, plastics, or common fabrics.

Ref.	Substrate	Material	ε_r	tan δ	Thickness (mm)	Frequency (GHz)
[9]	PCB	Taconic TLX-0	2.45	0.0019	0.787	2.0-2.5
		Taconic TF-290	2.90	0.0020	0.090	2.0-2.5
[10]		Taconic TLX-8	2.55	0.0019	0.127	6.0-12.0
[11]		ARLON AD-450	4.50	0.0020	1.580	1.9-2.2
[12]		F4BM	2.20	0.0007	1.000	2.0-10.0
[12]	Paper	Paper	2.25	0.0450	1.000	2.0-10.0
[12]	Plastic	PET	3.40	0.0700	1.000	2.0-10.0
[14]	Fabric	Nylon	2.40	0.0500	0.172	1.5-3.0
[15]		Cotton	2.10	0.0700	0.250	2.0
[15]		Fleece	1.35	0.0250	1.000	2.5-6.5

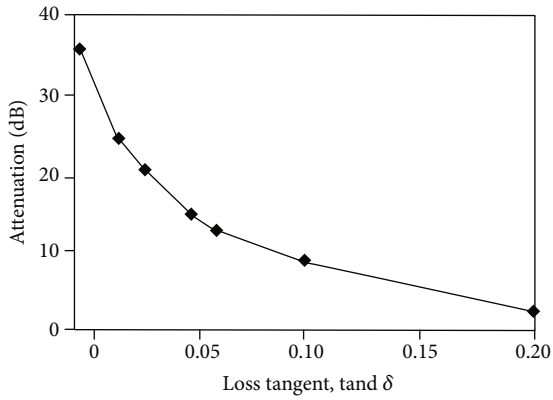

Figure 1: The relationship between attenuation and tan δ by simulation [13]. The attenuation decreased sharply at first and then slowly with the increase of tan δ.

the above researches indeed provided a foundation for the RF application of diverse flexible substrates. However, it still lacks a systematic research about how the dielectric properties of substrate materials affect the frequency response characteristics of the RF circuits.

Therefore, the theoretical calculation, simulation, and experimental verification methods were adopted in this research to systematically study the influence of dielectric properties on the RF performance of multiresonator. Firstly, the model of microstrip U-shaped multiresonators with the same substrate material was created in the Ansoft HFSS, and each of the resonant frequency and notch depth was compared with Reference [11] to prove the accuracy of our simulation. Then, the basic substrate parameters (ε_r, tan δ) were parametrically swept to explore the key parameters influenced on RF performances. Furthermore, three representative materials with different orders of magnitude of loss tangent were chosen to verify the simulated conclusions. They are Alron AD-450 with tan δ of 0.002 (lower loss), FR-4 with tan δ of 0.015 (medium loss), and denim fabric with tan δ of 0.114 (higher loss), respectively [16].

After all, the relationship between the dielectric loss and the RF performance of the multiresonant circuits was systematically analyzed in this research. It will offer guidance for designing wearable RF devices with lossy flexible materials, especially for textile materials with a wide range of dielectric losses.

2. Design and Optimization

The U-shaped resonator (also called hairpin resonator) is one of the basic units of multiresonating circuit for band-stop filtering. It consists of a microstrip line and a quarter-wavelength resonator. And the microstrip line feeds the resonators to form a weak coupling to modulate the spectrum of the interrogation signals. The resonant frequency and notch depth of the resonator significantly affect the filtering quality and capacity of information storage. The geometry structure and equivalent circuit are illustrated in Figure 2.

In Figure 2(b), the L and C are the equivalent shunt inductance and series capacitance, respectively. An N^{rd} multiresonant circuit consists of N U-shaped resonators. All resonators are coupled to the main microstrip line, and the coupling effect between each other is very weak and can be ignored by adjusting their distances.

The length of U resonator is determined according to Equation (1) [17], where each resonator resonates independently at its quarter-wavelength frequency ($\lambda g/4$). The effective dielectric constant is calculated by Equation (2) [18], and it is determined by the dielectric constant and thickness of the substrate as well as the width of the transmission line.

$$f_n = \frac{nc}{4(L + \Delta L)\sqrt{\varepsilon_{\text{eff}}(f)}}, \tag{1}$$

$$\varepsilon_{\text{eff}} = \frac{\varepsilon_r + 1}{2} + \frac{\varepsilon_r - 1}{2}\frac{1}{\sqrt{1 + (12h/w)}}, \tag{2}$$

$$Z_0 = \frac{60}{\sqrt{\varepsilon_{\text{eff}}}} \ln\left(\frac{8h}{w} + \frac{w}{4h}\right), \tag{3}$$

where f_n is the resonant frequency, n is the integer order of resonance, ε_{eff} is the effective dielectric constant, L is the length of the stub; ΔL is the extended equivalent length due to fringing field, c is the speed of light in free space, ε_r is

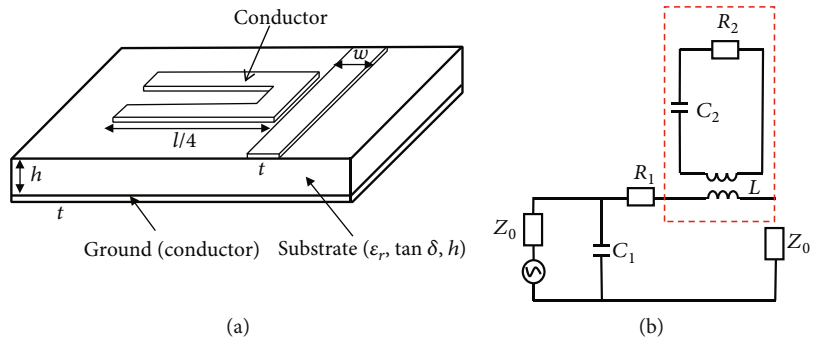

Figure 2: The structure of the microstrip U-shaped resonator: (a) the geometry of the basic unit and (b) the equivalent circuit. The U-shaped resonator is a quarter-wavelength resonator coupled to the microstrip line to form a parallel RLC resonant circuit.

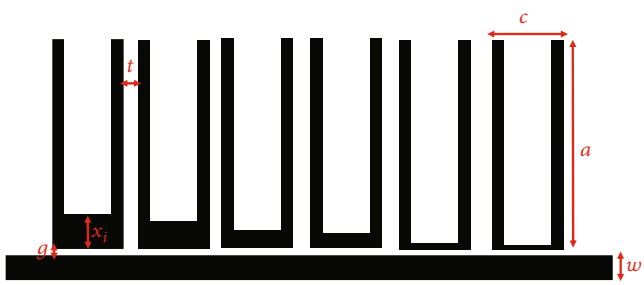

Figure 3: The layout of the designed U-shaped multiresonant circuit. It consists of six U-shaped resonators and a microstrip line.

Table 2: The dimension parameters of the above U-shaped multiresonator (unit: mm). They are determined by the performance of the filter, such as bandwidth, resonance frequency, and notch depth.

a	c	g	t	w	x_1	x_2	x_3	x_4	x_5	x_6
20	5.5	0.5	1.2	2.5	2.9	2.5	2.1	1.6	1.1	0.6

the dielectric constant of substrate, h is the thickness of the substrate, and w is the width of the transmission line.

Here, a designed prototype [11] was exploited to investigate the effect of substrate properties on the RF performance of microstrip multiresonant circuits. The layout of the designed multiresonator circuit is shown in Figure 3. And the geometric parameters of the hairpin multiresonator are listed in Table 2.

Based on the quarter-wavelength resonant principle, the length of the U-shaped arms (a) was calculated according to the resonant frequency and the dielectric constant of the substrate material. That is to say, for different materials, the resonant frequency would shift even if the geometric parameters of the resonator were the same. A series of parameters of "x_i" were designed to make each U resonator have a specific effective wavelength and resonate at its specific frequency. The distance between adjacent U-shapes (t) was determined by the optimized simulation to ensure almost no coupling between each U resonator. Therefore, according to the resonance frequency and bandwidth, the above three parameters can be preliminarily determined. Then, the distance between microstrip line and resonators (g) was adjusted to modulate the notch depth. Additionally, the width (w) of the transmission line was determined by the characteristic impedance (Equation (3) [18]), which was preferably to be 50Ω and equal to the input impedance of the antenna or the SMA connector.

The resonant model of multiresonator was established in Ansoft HFSS simulation software, according to the dimensions of Table 2. The substrate material was a commercial low-loss PCB and that is ARLON AD-450 with a dielectric constant of 4.5, loss tangent of 0.002, and thickness of 1.58 mm. The surface current distribution is shown in Figure 4. It can be seen that most of the current of the microstrip line was coupled to the branches of the resonators, resulting the notch effect. The simulated S-parameters of the multiresonator are shown in Figure 5.

This paper chose the classical U-shaped multiresonant circuit with the same dimensions and materials as Reference [11]. By simulation in HFSS, each resonant point and the corresponding S21 were compared with the reference, and the results are listed in Table 3. The results showed that the maximum frequency deviation was less than 2%, and the attenuation deviation was less than 9%, which indeed proved the accuracy of our simulation.

Then, the dielectric constant and loss tangent were parametrically sweeping, and their influences on the resonant frequency and notch depth were discussed. The results of the simulation are listed in Figure 6.

Figure 6(a) is the influence of dielectric constant on the resonant frequency and attenuation of U-shaped multiresonators. The resonant curve shifts from right to left, but the overall shape remains the same. The bigger the dielectric constant, the smaller the resonant frequency. The simulation results show that the dielectric constant has no appreciable effect on the notch depth, only changing the resonant frequency. Figure 6(b) is the influence of dielectric loss tangent on the resonant frequency and attenuation of U-shaped multiresonators. All resonant frequencies remain the same, while the notch depths vary with each other. Within a certain range, with the increase of tan δ, the notch depth decreases sharply. When the tan δ is larger than 0.2, the notch effect is disappeared and the multiresonators cannot achieve the purpose of filtering. From the above simulation, it can be concluded that the tan δ of the substrate plays a decisive role in the depth of the notch.

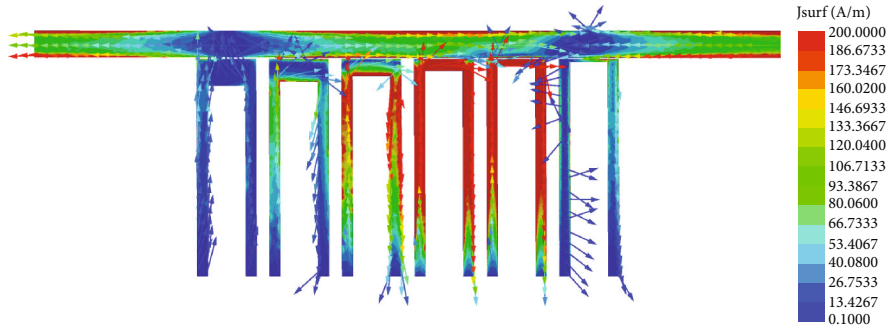

Figure 4: The distribution of surface current of the multiresonator circuit. Most of the current of the microstrip line was coupled to the branches of the resonators. This is the reason that notch effect occurs.

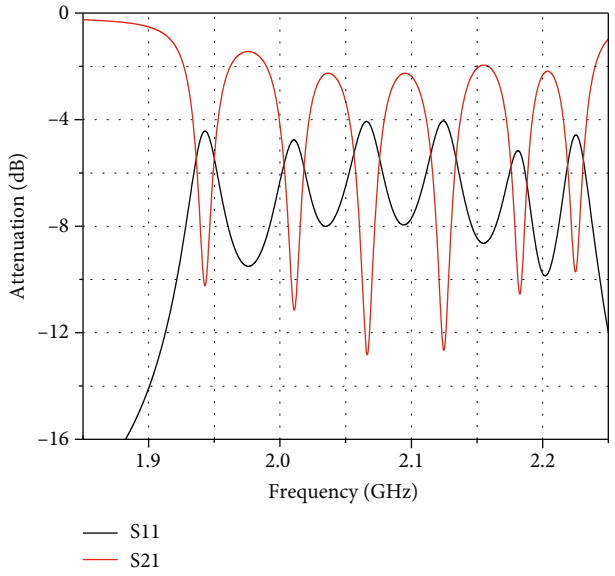

Figure 5: Simulated *S*-parameters of the multiresonator based on ARLON AD-450 substrate. Obviously, there are six notch depths evenly distributed within the bandwidth of 1.9 GHz~2.3 GHz, indicating a good filtering performance.

3. Experiment and Measurement

3.1. Experiment. In this research, three kinds of substrate materials (ARLON AD-450 PCB, FR-4 PCB, and common denim fabric) were chosen as the substrate materials to investigate the influence of substrate material properties on RF performance of multiresonant circuits (as shown in Figure 7). The dielectric properties of these substrates are measured by the split post dielectric resonators (Keysight Technologies, Inc.). And the key parameters are listed in Table 4.

For AD-450 PCB (Figure 7(a)), the multiresonator was customized by an electronic technology company (Hontec Quick Electronics Limited). The substrate material was low-loss ARLON AD-450 PCB with a dielectric loss tangent of 0.002.

For FR-4 PCB (Figure 7(b)), the resonator was fabricated by a traditional etching process. Firstly, the filter structure was printed on paper by a normal inkjet printer. And then, the layout of the resonator was transferred to the surface of the PCB by iron at high temperature. As a result, a layer of toner was firmly fixed to a specific position on the surface of the copper film. Thus, during the acid corrosion process, the structure covered with the toner is protected, while the copper film in other areas would be removed. The copper film of FR-4 was corroded by acid $FeCl_3$ solution (H_2O : $FeCl_3$ = 1 : 10). The redox reaction lasted 20 minutes at 40~50°C. The last process was to rinse and dry in the oven.

For denim fabric substrates (Figure 7(c)), the copper tape was pasted on the common denim fabric, and the pattern of the multiresonator was cut out. This process has certain defects with a certain deviation about the dimensions of the multiresonator during the manual fabrication.

3.2. Measurement. As one of the typical circuits within the RF applications, the resonant frequency and notch depth affect the filtering quality and information storage of modulated signals. In this research, the resonant frequency and notch depth of the multiresonators were measured and compared with the simulated results.

For the measurement, firstly, the multiresonator was mounting to the SMA connectors connecting with two ports of the Agilent E5071C ENA (as shown in Figure 8). Secondly, the full two-port calibration was done with Calibration Kit (Agilent 85052D (3.5 mm)) before the measurement to eliminate the instrument errors. Then, the sample was measured and the relation curves of resonant frequency and S21 were exported. The measured and simulated results of the 3 kinds of multiresonators are shown in Figures 9, 10, and 11, respectively.

4. Results and Discussions

The first step of this research was to demonstrate the accuracy of our simulation. The resonant model of multiresonator was established in Ansoft HFSS simulation software, and all materials and dimensions were identical with Reference [11]. By simulation, each resonance point and the corresponding S21 were compared with the reference (as listed in Table 3). After calculation, the maximum frequency shift was less than 2%, and the maximum notch depth shift was less than 9%. It proved the accuracy of the simulated methods and results, and the slight deviation should be caused by the difference of meshing accuracy during the simulation.

Table 3: The simulated results were compared with the literature [11]. Each resonant point and the corresponding S21 were compared with the reference, and the deviation was small to indicate the accuracy of the simulation.

Type	Resonant point	1	2	3	4	5	6
Frequency (GHz)	Ref. [11]	1.90	1.97	2.03	2.10	2.17	2.22
	This work (simulation)	1.94	2.01	2.06	2.12	2.18	2.23
S21 (dB)	Ref. [11]	-11.00	-12.20	-11.80	-12.20	-10.00	-9.60
	This work (simulation)	-10.20	-11.20	-12.80	-12.70	-10.60	-9.60

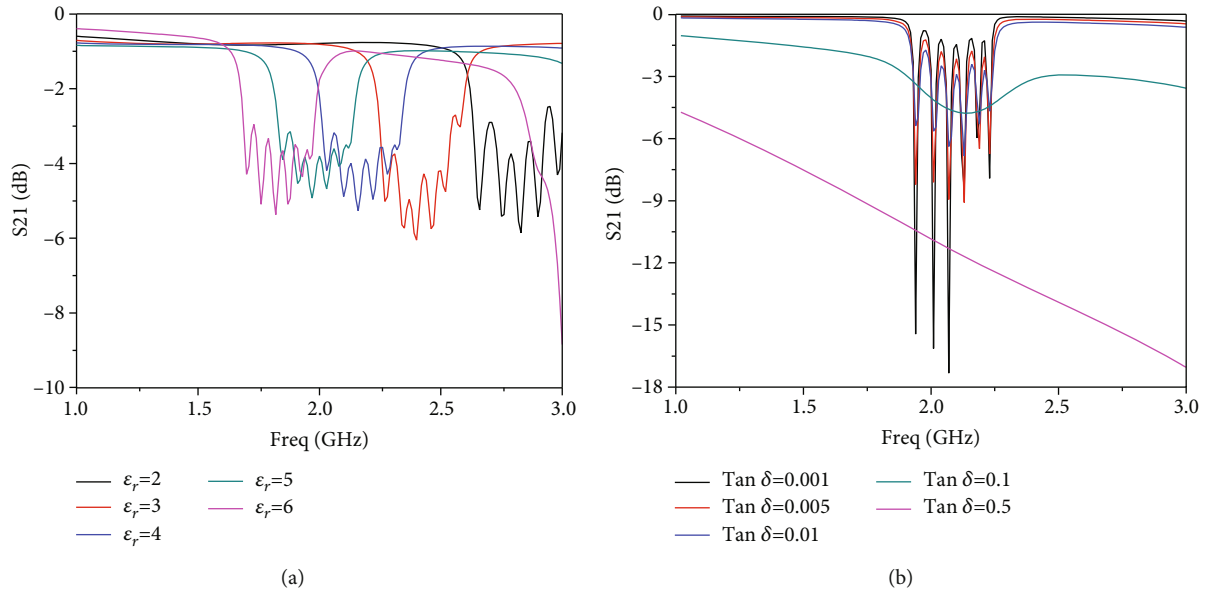

Figure 6: The influence of dielectric constant and loss tangent on RF performance: (a) increase dielectric constant (tan $\delta = 0.02$) and (b) increase dielectric loss tangent ($\varepsilon_r = 4.5$). The simulation results show that the dielectric constant only affects the resonant frequency, and the loss tangent significantly affects the notch depth.

On the other hand, by parametrically sweeping, it has showed that the dielectric loss tangent was the key factor for the notch depth. The larger the tan δ, the bigger the electromagnetic loss of the material, resulting in a smaller notch depth of the resonator. Then, three multiresonators based on AD-450 (tan $\delta = 0.002$), FR-4 (tan $\delta = 0.015$), and denim fabric (tan $\delta = 0.114$) were fabricated to verify the conclusions of the simulation.

For multiresonator based on ARLON AD-450 PCB (Figure 9), there are 6 sharp dips almost evenly distributed in the frequency range of 1.90 GHz~2.20 GHz. And the notch depths are in the range of -5 dB to -10 dB. The points of resonant frequency are 1.88 GHz, 1.84 GHz, 2.01 GHz, 2.07 GHz, 2.13 GHz, and 2.18 GHz, respectively. The maximum frequency shift of measured results is about 0.04 GHz compared to the simulation. The overall resonant frequency offset rates are less than 2%, which considered reasonable because the radiation and environmental disturbances were ignored in the ideal electromagnetic field of the simulation. The measured and simulated curves of the multiresonator based on ARLON AD-450 PCB are almost coincident with each other. It shows that the multiresonant circuit based on the ARLON AD-450 has the best filtering effect. The main difference between the simulated and measured results is that the simulation is an ideal electromagnetic field, ignoring the radiation loss.

For multiresonator based on FR-4 PCB (Figure 10), there are also 6 obvious dips almost evenly distributed in the frequency range of 1.90 GHz~2.20 GHz. However, there is a large deviation between the simulated and the measured curves for FR-4 PCB, which may be the inconsistent dielectric properties of the FR-4 materials from different batches or manufacturers. In addition, the dips are less sharper than those multiresonators of ARLON AD-450 PCB (Figure 9). The main reason is that the material FR-4 has a larger loss tangent than ARLON AD-450 PCB, and there are many energy wastes inside the substrate during the signal transmission. Therefore, for the same resonator, the dielectric loss of the substrate material has a great influence on the notch depth, which in turn affects the RF performance of the filter.

For multiresonator based on common denim fabric (Figure 11), there is no obvious resonant effect during the whole resonant zone compared with the other two multiresonators based on the materials of AD-450 and FR-4 (Figures 9 and 10). In Figure 11, there are some jitters in the measured curve of S21, which should theoretically be lower than the simulated curve. This may be caused by the following reasons. On

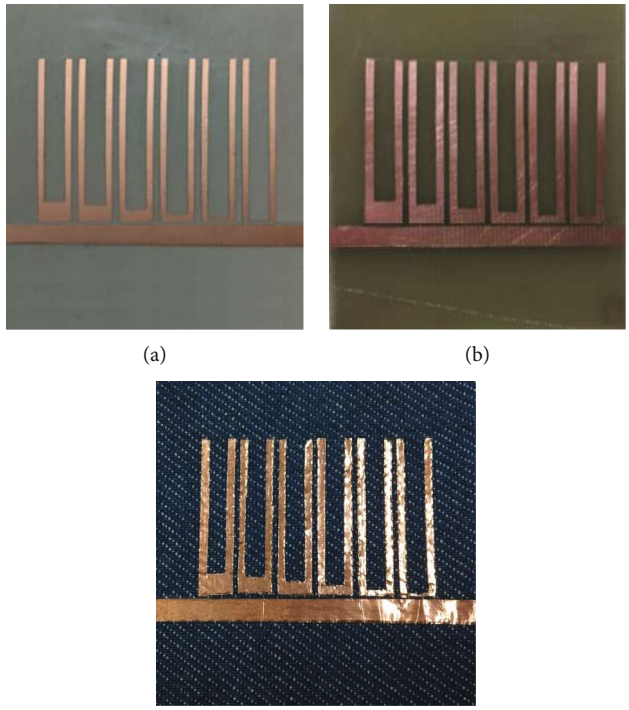

(a) (b)

(c)

Figure 7: The fabricated multiresonators on different substrates: (a) ARLON AD-450, (b) FR-4, and (c) common denim fabric. The geometric parameters of the multiresonators are the same.

Table 4: The key parameters of the above three kinds of substrates. The values of tan δ are larger than the one order of magnitude from each other.

Types	Parameter	(a)	(b)	(c)
Substrate	Materials	ARLON AD-450	FR-4	Denim fabric
	Dielectric constant (ε_r)	4.50	5.20	2.16
	Loss tangent (tan δ)	0.002	0.015	0.114
	Thickness (mm)	1.58	1.50	0.56
Conductor	Materials	Copper	Copper	Copper
	Thickness (mm)	0.035	0.018	0.018

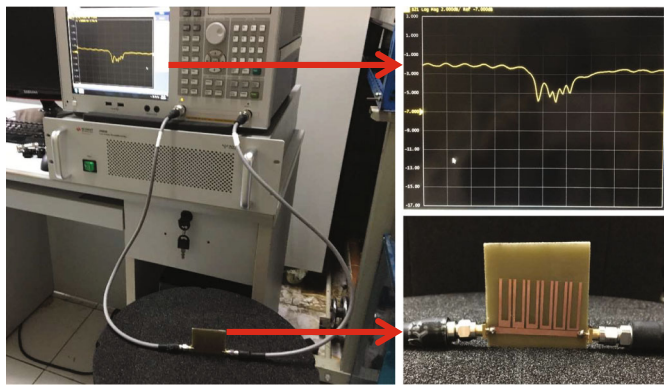

Figure 8: The measurement of RF performance for the multiresonant circuit (FR-4 PCB). The resonator was mounted to the SMA connectors of the two ports of the ENA. The frequency response characteristics were obtained by this measurement.

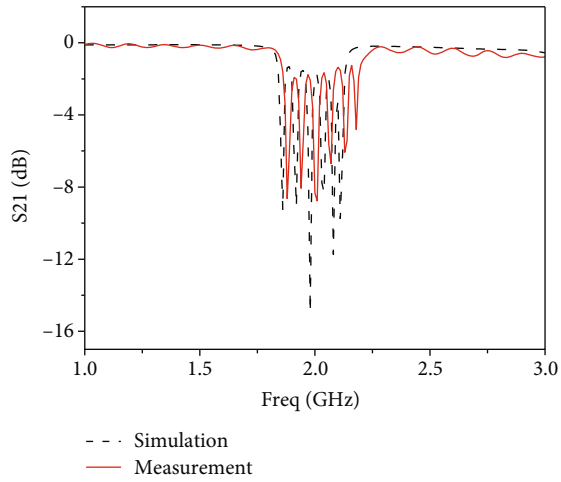

Figure 9: The measured and simulated *S*-parameters of the multiresonator based on ARLON AD-450 PCB. There are six notch depths evenly distributed within the bandwidth, and the measured and simulated curves are almost coincident with each other, indicating a good filtering performance.

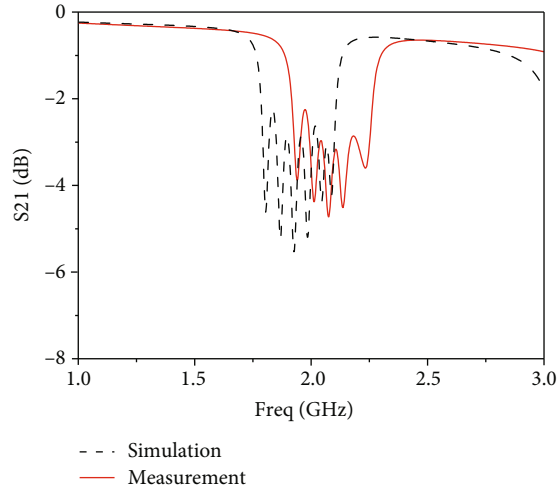

Figure 10: The measured and simulated *S*-parameters of the multiresonator based on FR-4 PCB. There is a large deviation between the simulated and the measured curves, and the notch depth is less sharper than that of ARLON AD-450 PCB.

the one hand, it is not accurate to use the fabric as a homogeneous material in the simulation with specific dielectric properties due to the large porosity in the fabric. On the other hand, the principle of notch depth is that a quarter-wavelength U-shaped resonator is coupled to the microstrip line to form a parallel RLC resonant circuit, which is a weak coupling effect. As the denim fabric has a very large loss tangent (larger than 0.1), most of the energy wastes are inside the substrate during the signal transmission. Thus, the coupling disappears and no filtering effect.

Generally, for a resonant circuit, the loss mainly divides into three categories, and they are bulk loss, dielectric loss, and radiation loss, respectively (Equation (4) [19]). Among them, the conductor loss is closely related to the surface

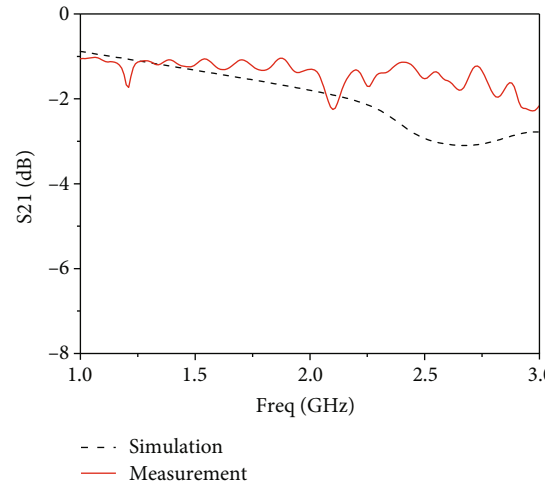

Figure 11: The measured and simulated *S*-parameters of the multiresonator based on denim fabric. No notch effect indicates that this resonator cannot achieve effective filtering.

Table 5: Parameters of the substrates used in fabric-based RF devices. It shows that the dielectric loss tangents of fabric materials vary widely.

Ref.	Substrate material	ε_r	tan δ	Thickness (mm)	Frequency (GHz)
[Here]	Denim fabric	2.16	0.114	0.560	1.0-3.0
[20]	Cotton	1.71	0.020	1.090	2.0-2.8
[21]	Cotton/PES	1.64	0.028	2.808	2.0-3.0
[22]	PET	1.20	0.020	1.000	2.45
[23]	Polyamide 66	1.90	0.0098	0.500	2.45
[24]	Kevlar fabric	2.60	0.006	0.590	0.1-1.0

resistance of the conductor. The dielectric loss is proportional to the dielectric loss tangent of the substrate material. The radiation loss is usually affected by the conductivity and skin depth of the metal conductor.

$$\alpha_{\text{total}} = \alpha_c + \alpha_d + \alpha_r, \tag{4}$$

where $\alpha_c \propto R(f) \times \sqrt{\varepsilon_r}$, $R(f)$ is the surface resistance; $\alpha_d \propto f \times \tan\delta \times \sqrt{\varepsilon_r}$, f is the resonant frequency; and $\alpha_r \propto (1/\sqrt{\pi\mu\sigma f})$, σ is the conductivity of the conductor.

The conductor materials of these three resonators are copper, although the thickness is different. However, at 2 GHz, the theoretical skin depth is 1.5 μm after calculation. As the thickness of the copper films (18 μm) is much larger than 3 times of the theoretical skin depth, it does not affect the conductor loss. Therefore, for these three resonators with different substrate materials, the conductor loss and radiation loss are exactly the same, and the difference of RF performance of these multiresonators is only the conduct by the dielectric loss of the substrates.

Table 5 is the parameters of the substrate used in fabric-based RF devices. It shows that the dielectric loss tangents of common fabrics for clothing are very large (above 0.01), and for new high-performance fabrics such as polyamide or aramid, the dielectric loss tangents are as small as the commercial low-loss PCBs (as shown in Table 1). The dielectric loss of denim fabric in this research is one to two orders of magnitude larger than that of commercial PCBs. As a result, no filtering effect achieves. Therefore, it is of great significance to choose appropriate materials for the designs.

5. Conclusion

In this research, theoretical calculation, simulation, and experiments were carried out to systematically discuss the influence of dielectric loss on the RF performance of U-shaped multiresonators. The results show that the dielectric constant can only change the resonance frequency while the dielectric loss tangent is the key factor for the notch depth of resonant circuits. The bigger the tan δ, the weaker the notch depth, resulting in a bad filtering quality. Most common fabrics for clothing with big dielectric loss are not suitable for the substrate materials of multiresonant circuits. Lower loss fabrics made of high-performance synthetic fibers such as polyamide and aramid (Kevlar®) are expected to be chosen if properly designed. In all, this paper provides guidance for the material selection or development of fabric-based flexible electronic devices.

Data Availability

The [DATA TYPE] data used to support the findings of this study are included within the article.

Conflicts of Interest

No potential conflict of interest was reported by the authors.

Acknowledgments

This work was financially supported by the Shanghai High Level University Construction Project (E1-2602-21-201006-1), the Foundation of Shanghai Intelligent Medical Devices and Active Health Collaborative Innovation Center, and the Three-Year Action Plan for Key Discipline Construction Project of Shanghai Public Health System Construction (Project No. GWV-10.1-XK05).

References

[1] A. Leal-Junior, L. Avellar, A. Frizera, and C. Marques, "Smart textiles for multimodal wearable sensing using highly stretchable multiplexed optical fiber system," *Scientific Reports*, vol. 10, article 13867, 2020.

[2] S. Yang, C. Li, N. Wen et al., "All-fabric-based multifunctional textile sensor for detection and discrimination of humidity, temperature, and strain stimuli," *Journal of Materials Chemistry C*, vol. 9, no. 39, pp. 13789–13798, 2021.

[3] A. T. Singh, D. Lantigua, A. Meka, S. Taing, M. Pandher, and G. Camci-Unal, "Paper-based sensors: emerging themes and applications," *Sensors (Basel)*, vol. 18, article 2838, no. 9, 2018.

[4] H. Tai, Z. Duan, Y. Wang, S. Wang, and Y. Jiang, "Paper-based sensors for gas, humidity, and strain detections: a review," *ACS Applied Materials & Interfaces*, vol. 12, no. 28, pp. 31037–31053, 2020.

[5] Z. Wu, F. Yang, J. Yang et al., "Durable and flexible PET-based bending sensor obtained by immobilizing carbon nanotubes via surface micro-dissolution for body motion monitoring," *Macromolecular Materials and Engineering*, vol. 307, no. 1, article 2100502, 2022.

[6] R. Garg, *Microstrip Antenna Design Handbook*, Artech House, United States, 2001.

[7] F. Bashore, "CAD of microstrip antennas for wireless applications," in *Artech House*, United States, 1996.

[8] J. C. Yves-Thierry, U. Vichate, and J. A. Barbosa, "Effects of substrate permittivity on planar inverted-F antenna performances," *Journal of Computers*, vol. 4, no. 7, pp. 610–614, 2009.

[9] S. Preradovic, *Chipless RFID system for barcode replacement, [Ph.D. thesis]*, Monash University, Australia, 2017.

[10] M. S. Bhuiyan and N. C. Karmakar, "An efficient coplanar retransmission type chipless RFID tag based on dual-band MCSRR," *Progress in Electromagnetics Research C*, vol. 54, pp. 133–141, 2014.

[11] G. A. Casula, G. Montisci, P. Maxia, and G. Mazzarella, "A narrowband chipless multiresonator tag for UHF RFID," *Journal of Electromagnetic Waves and Applications*, vol. 28, no. 2, pp. 214–227, 2014.

[12] B. Shao, C. Qiang, Y. Amin, R. Liu, and L. Zheng, "Chipless RFID tags fabricated by fully printing of metallic inks," *Annals of Telecommunications*, vol. 68, no. 7-8, pp. 401–413, 2013.

[13] M. A. Islam and N. C. Karmakar, "Real-world implementation challenges of a novel dual-polarized compact printable chipless RFID tag," *IEEE Transactions on Microwave Theory & Techniques*, vol. 63, no. 12, pp. 4581–4591, 2015.

[14] H. Tu, Y. Zhang, H. Hong, J. Hu, and X. Ding, "Design and characterization of novel fabric-based multi-resonators for wearable chipless RFID applications," *Textile Research Journal*, vol. 91, no. 15-16, pp. 1830–1840, 2021.

[15] A. Vena, E. Moradi, K. Koski, A. Babar, and M. Tentzeris, "Design and realization of stretchable sewn chipless RFID tags and sensors for wearable applications," in *2013 IEEE International Conference on RFID (RFID)*, pp. 176–183, Orlando, FL, USA, April 2013.

[16] http://altium.com/p/increasingly-important-role-loss-tangents-pcb-laminates.

[17] Y. H. Chou, M. J. Jeng, Y. H. Lee, and Y. G. Jan, "Measurement of RF PCB dielectric properties and losses," *Progress in Electromagnetics Research Letters*, vol. 4, pp. 139–148, 2008.

[18] S. Sankaralingam and B. Gupta, "Determination of dielectric constant of fabric materials and their use as substrates for design and development of antennas for wearable applications," *IEEE Transactions on Instrumentation & Measurement*, vol. 59, no. 12, pp. 3122–3130, 2010.

[19] E. J. Denlinger, "Losses of microstrip lines," *IEEE Transactions on Microwave Theory and Techniques*, vol. 28, no. 6, pp. 513–522, 1980.

[20] C. Hertleer, A. V. Laere, H. Rogier, and L. V. Langenhove, "Influence of relative humidity on textile antenna

performance," *Textile Research Journal*, vol. 80, no. 2, pp. 177–183, 2010.

[21] M. L. Scarpello, I. Kazani, C. Hertleer, H. Rogier, and D. V. Ginste, "Stability and efficiency of screen-printed wearable and washable antennas," *IEEE Antennas and Wireless Propagation Letters*, vol. 11, pp. 838–841, 2012.

[22] I. Ullah, M. Wagih, and S. P. Beeby, "Design of textile antenna for moisture sensing," *Engineering Proceedings*, vol. 15, no. 11, pp. 1–4, 2022.

[23] C. Loss, C. Lopes, R. Salvado, R. Gonçalves, and P. Pinho, "Smart coat with a textile antenna for electromagnetic energy harvesting," 2015.

[24] J. Zhong, A. Kiourti, T. Sebastian, Y. Bayram, and J. L. Volakis, "Conformal load-bearing spiral antenna on conductive textile threads," *IEEE Antennas and Wireless Propagation Letters*, vol. 16, pp. 230–233, 2017.